HHS Public Access

Author manuscript

Prostate. Author manuscript; available in PMC 2015 April 18.

Published in final edited form as:

Prostate. 2012 March ; 72(4): 437–449. doi:10.1002/pros.21445.

Altered Prostate Epithelial Development in Mice Lacking the Androgen Receptor in Stromal Fibroblasts

Shengqiang Yu[1], **Chiuan-Ren Yeh**[1], **Yuanjie Niu**[1,2], **Hong-Chiang Chang**[1,3], **Yu-Chieh Tsai**[1,2], **Harold L Moses**[4], **Chih-Rong Shyr**[1,5], **Chawnshang Chang**[1,5,*], and **Shuyuan Yeh**[1,*]

[1]George Whipple Lab for Cancer Research, Departments of Pathology and Urology, The Wilmot Cancer Center, University of Rochester Medical Center, Rochester, New York

[2]Chawnshang Chang Sex Hormone Research Center, Tianjin Institute of Urology, The 2 nd Hospital of Tianjin Medical University, Tianjin, China

[3]Departments of Urology and Oncology, National Taiwan University/Hospital, Taipei, Taiwan

[4]Department of Cancer Biology and Urology, Vanderbilt University, Nashville, Tennessee

[5]Sex Hormone Research Center, China Medical University & Hospital, Taichung, Taiwan

Abstract

BACKGROUND—Androgens and the androgen receptor (AR) play important roles in the development of male urogenital organs. We previously found that mice with total AR knockout (ARKO) and epithelial ARKO failed to develop normal prostate with loss of differentiation. We have recently knocked out AR gene in smooth muscle cells and found the reduced luminal infolding and IGF-1 production in the mouse prostate. However, AR roles of stromal fibroblasts in prostate development remain unclear.

METHODS—To further probe the stromal fibroblast AR roles in prostate development, we generated tissue-selective knockout mice with the AR gene deleted in stromal fibroblasts (FSP-ARKO). We also used primary culture stromal cells to confirm the in vivo data and investigate mechanisms related to prostate development.

RESULTS—The results showed cellular alterations in the FSP-ARKO mouse prostate with decreased epithelial proliferation, increased apoptosis, and decreased collagen composition. Further mechanistic studies demonstrated that FSP-ARKO mice have defects in the expression of prostate stromal growth factors. To further confirm these in vivo findings, we prepared primary cultured mouse prostate stromal cells and found knocking down the stromal AR could result in growth retardation of prostate stromal cells and co-cultured prostate epithelial cells, as well as decrease of some stromal growth factors.

*Correspondence to: Chawnshang Chang and Shuyuan Yeh, George Whipple Lab for Cancer Research, Departments of Pathology and Urology, The Wilmot Cancer Center, University of Rochester Medical Center, Rochester, NY 14642. chang@urmc.rochester.edu, shuyuan_yeh@urmc.rochester.edu.

Shengqiang Yu, Chiuan-Ren Yeh, and Yuanjie Niu contributed equally to this work.

Conflicts of Interest: None.

CONCLUSIONS—Our FSP-ARKO mice not only provide the first in vivo evidence in Cre-loxP knockout system for the requirement of stromal fibroblast AR to maintain the normal development of the prostate, but may also suggest the selective knockdown of stromal AR might become a potential therapeutic approach to battle prostate hyperplasia and cancer.

Keywords

androgen receptor; prostate; fibroblast specific protein; epithelium; Cre-loxP

INTRODUCTION

The androgen receptor (AR) plays a central role in the normal prostate development and cancer progression [1–3], and men or mice without functional AR fail to develop prostate [4, 5]. AR was detected in the stromal and epithelial cells of prostate, and the androgenic effects on prostatic development are mediated via the AR in the context of mesenchymal–epithelial interactions [6, 7]. The important relationship of AR in mesenchymal–epithelial interactions is revealed by the ontogeny of AR in the prostate. During prenatal development, AR is initially detected solely in the urogenital sinus mesenchyme (UGM) prior to and during prostate bud formation, and is undetectable in the epithelial compartment [8], which suggests that mesenchymal AR, but not epithelial AR, is critically involved in the early phases of prostate development.

Furthermore, mice with tissue recombinant inoculation composed of wild type (WT)-UGM and WT-epithelium formed prostates in response to androgens [9, 10]. In contrast, the mice with tissue recombinants composed of testicular feminization (Tfm)-UGM and WT-epithelium failed to form prostates even in the presence of androgens, suggesting a critical role of mesenchymal AR in the initiation of prostatic ductal morphogenesis and epithelial cytodifferentiation [9, 10]. Cunha's group and Mizuno's group [11] have made contributions in the studies of AR roles in the prostate development using tissue recombination experiments.

It is known that the prostate stroma is not homogeneous and contains multiple cell types, including the fibroblast cells, smooth muscle cells (SMCs), inflammatory cells, nerve cells, and blood vessels. The tissue recombination assay can only study the AR roles in the UGM and its differentiated cells, yet cannot dissect AR roles in different stromal cell types in the prostate microenvironment and in immune intact mice. The advantage of the Cre-loxP system is to knock out AR in a selective cell type, which allows us to study the AR roles in fibroblasts and its consequent impacts on prostate development through adult stage in an in vivo setting.

Our previous study has shown that total ARKO male mice failed to develop prostate [5], but the prostate epithelial specific ARKO (pes-ARKO) mice developed prostates with loss of cell differentiation with an increased basal-intermediate cell population and decreased luminal epithelial cells [12]. We further studied the stromal AR roles in the prostate development in early and late adult stages via knocking out AR in SMCs, and found defects in prostate development with decreased expression of IGF-1 [13]. In the current study, we focused on delineating AR roles in the prostate stromal fibroblasts. By mating the floxed AR

mice [5] with transgenic mice possessing fibroblast specific protein 1 (FSP1) promoter-driven expression of the Cre recombinase [14, 15], we obtained male mice with the AR gene selectively deleted in prostate stromal fibroblast cells (FSP-ARKO). Analyses of the FSP-ARKO mice revealed altered prostate development with normal serum testosterone levels. Mechanistic studies suggested that the defects of stromal cell secretary factors rendered by knockout of stromal fibroblast AR may contribute to the alteration in the prostate development. The primary cultured prostate stromal cells were also applied to confirm the in vivo findings.

MATERIALSANDMETHODS

Generation of Prostate FSP-ARKO Mice

To generate the FSP-ARKO mice and WT littermates, transgenic male mice (C57BL/6) expressing Cre recombinase under the control of the mouse FSP1 promoter [14, 15] were mated with floxed AR (C57BL/6) female mice [5]. We genotyped 21-day-old pups from tail snips by polymerase chain reaction (PCR) as described previously [5]. FSP-ARKO mice expressed floxed AR and Cre alleles in tail genomic DNA (Fig. 1A). Protocols for use of animals were in accordance with the National Institutes of Health standards.

RNA Extraction, Reverse Transcriptase-PCR (RT-PCR), and Real-Time Quantitative PCR (Q-PCR)

Total RNA was extracted and purified using Trizol (Invitrogen, Carlsbad, CA) according to the manufacturer's instructions. Three microgram total RNA was subjected to reverse transcription using Superscript III (Invitrogen). RT-PCR has been described previously [16], using primers designed from AR exon 1 and exon 3: AR sense, 5′-TATCCTGGTGGAGTTGTG-3′; AR antisense, 5′-CAGAGTCATCCCTGCTTC-3′. Q-PCR was performed with cDNA, specific gene primers (Table I), and SYBR Green PCR Master Mix (Biorad, Hercules, CA) as described previously [17]. All samples were run in triplicate. Data were analyzed using iCycler iQ software (Biorad), and the values were normalized by the 18S levels.

Immunohistochemistry (IHC), Hematoxylin and Eosin (H&E), and Immunofluorescence (IF) Staining

For the IHC staining, the detailed procedure was described previously [18]. The following primary antibodies: Anti-AR (C-19, Santa Cruz sc-815, 1:400), anti-Ki67 (NCL-Ki67p, 1:1,000), and anti-β-galactosidase (β-Gal) (40-1A, Iowa Hybridoma Bank, 1:300) were used. For the H&E staining, the sections were stained in hematoxylin for 5 min, and washed in running tap water for 5 min, then stained in eosin for 30 sec, dehydrated, and mounted. For the IF staining, the chamber slides with attached cells were incubated with the following antibodies: anti-vimentin (Sigma, 1:200), anti-smooth muscle alpha-actin (SMA) (Sigma, 1:200), and IgG control in 3% BSA overnight at 4°C, then incubated with 1:200 diluted fluorescence-labeled secondary antibodies (Invitrogen, 1:300) for 1 hr at room temperature, and mounted by mounting medium containing 4′,6-diamidino-2-phenylindole (DAPI) (Vector Laboratories).

Apoptosis Measurement Using TUNEL Assay

Apoptosis was detected by TUNEL assay [19] following the manufacturer's suggested protocol (Roche Pharmaceuticals). For the positive controls, we incubated sections with DNase I (3,000 U/ml in 50 mM Tris–HCl pH 7.5, 100 μg/ml BSA) for 10 min at 15–25°C. For the negative controls, we incubated sections with label solution (without terminal transferase) instead of TUNEL reaction mixture.

Assessment of Serum Testosterone Levels

Male FSP-ARKO mice and their WT littermates were sacrificed at 24 weeks. After anesthesia (100 μg Nembutal/g of body weight), 1 ml blood sample was collected by cardiocentesis, and centrifuged at 3,000g for 15 min to collect the serum. Then the total serum testosterone levels were measured by Testosterone enzyme immunoassay (EIA) kits (DSL-10-4000, Diagnostic Systems Laboratories, Inc) according to the manufacturer's suggested protocol. Duplicate assays were performed for each serum sample.

Culture of Mouse Stromal Cells

The mouse prostate stromal cells (PrSCs) were primary cultured from WT male mice (C57BL/6). The mouse prostates were cut into small pieces (1 mm^3), then were digested with type I collagenase (2.8 mg/ ml; Sigma) and hyaluronidase (1 mg/ml; Sigma) in RPMI 1640 at 37°C for 8 hr. Then the stromal and epithelial cells were separated by discontinuous Percoll gradient method [20]. The isolated PrSCs were cultured with RPMI 1640 medium (with 10% fetal bovine serum) in 5% CO_2 37°C incubator. Then the PrSCs were infected by lentivirus containing AR-siRNA [21] or scramble sequence to establish the PrSC-ARsi and control PrSC-sc cells, respectively.

Methyl Thiazolyl Tetrazolium (MTT) Assay and Cell Co-Culture Assay

2×10^4 stromal cells were seeded in 24-well plates and incubated with RPMI medium with 10% fetal bovine serum. The plates were stained with MTT (Sigma) at day 0, 2, 4, 6 for 3 hr, and the absorbency was read at a wavelength of 575 nm. For the cell coculture assay, we used the 1 μm transwell system from BD Biosciences following the manufacturer's suggested protocol. Briefly, 1×10^5 stromal cells in 0.5 ml RPMI medium (with 2% fetal bovine serum) were seeded into the lower chamber, and 5×10^3 BPH-1 cells in 0.75 ml of same medium were put into the upper chamber. The stromal cells in lower chambers were changed every 2 days. The upper chamber was stained with MTT as described above.

Masson's Trichrome Staining

The tissue sections were stained by the Masson's trichrome staining kit (Sigma, HT15) following the manufacturer's protocol. The positive signals were quantified with Image J (HIN) software [22]. Briefly, the image colors were separated into RED, GREEN, and BLUE parts; the values were calculated by "BLUE – RED – GREEN" and normalized by the length of prostate basement membrane.

Picrosirius Red Staining

The tissue sections were stained by the Picrosirius red staining kit (Polysciences Inc., 24901) following the manufacturer's protocol. The positive signals were quantified with Image J (HIN) software [22], similar to the Masson's trichrome staining. The only difference is the values were calculated by "RED – BLUE – GREEN."

Statistical Analyses

Values were expressed as mean × standard deviation (S.D.). We used the Student's *t* test to compare values between the two groups. Calculated *P* values were two-sided, and $P < 0.05$ was considered statistically significant.

RESULTS

Generation of Mice with Conditional Knockout of AR in Prostate Stromal Fibroblasts

Using a Cre-loxP conditional knockout strategy, we mated female heterozygous floxed AR mice with male FSP-Cre mice to generate FSP-ARKO and WT male littermates. We were able to detect Cre and floxed AR DNA fragments in tail genomic DNA of 3-weeks-old FSP-ARKO mice (Fig. 1A). In addition, RNAs from different prostate lobes, ventral (VP), dorsolateral (DLP), and anterior (AP), were harvested from adult FSP-ARKO and WT mice at 12 weeks. All three lobes showed deletion of AR exon 2 with a 220 bp signal from RT-PCR using primers from exon 1 and exon 3 of AR (Fig. 1B). The remaining WT bands are due to the WT AR in epithelial cells and stromal cells other than fibroblasts, including smooth muscle, endothelia, and neuron cells.

Cre recombination was further confirmed by breeding the FSP-Cre mice with the ROSA26r-β-Gal mouse, which harbors a bacterial β-Gal cDNA reporter gene, and its expression relies on the deletion of the loxP-flanked "stop" sequence that separates the ROSA26 promoter and the β-Gal gene. Thus, the β-Gal gene can be expressed where Cre is expressed and activated. As expected, prostate stromal cells show efficient recombination and intensive staining, and the epithelial cells have no staining signal. Compared to AP and DLP, the VP has higher β-Gal expression levels, which indicate the higher Cre activity in VP (Fig. 1C). Furthermore, no positive staining was found in ROSA26r-β-Gal, Cre-negative control mice. IHC staining was also applied to confirm that the loss of AR was dominant and selective in prostate stromal cells (Fig. 1D). Together, results from genomic DNA genotyping, prostate mRNA RT-PCR detection, and IHC staining all revealed that the AR gene was selectively knocked out in prostate stromal cells of FSP-ARKO mice.

Altered Prostate Epithelial Structure in FSP-ARKO Mice with Normal Serum Testosterone Level

The gross appearance of FSP-ARKO and WT mouse prostates is similar (Fig. 2A). But by weighing each lobe of the prostate, we found the VPs of FSP-ARKO mice were lighter than those in WT littermates, which is consistent with our observation of higher FSP-Cre activity in VPs (Fig. 2B, $P < 0.05$). We then examined the histology of VPs from 6-, 12-, and 24-weeks-old, and found no obvious change in 6-weeks-old FSP-ARKO mice, but less epithelial folding structures were observed in some prostate ducts of FSP-ARKO mice

compared to WT littermate prostates of 12-weeks-old. In the 24-week-old mice, we observed changed epithelial cells with more cuboidal and flattened shapes in prostate ducts of FSP-ARKO mice; as a comparison, the WT prostate epithelial cells remain columnar shape (Fig. 2C). Our data suggested the reduced epithelial differentiation in prostates of FSP-ARKO at later adult stage. To rule out the possibility of the serum testosterone influence, we determined the serum testosterone levels by ELISA assay and found no significant difference between FSP-ARKO mice and WT littermates (Fig. 2D). Furthermore, there were little changes of the SV weight (Fig. 2B), total body weight, testis weight, epididymis weight, and sperm numbers (data not shown) between FSP-ARKO mice and their WT littermates.

Reduced Proliferation and Increased Apoptosis in the FSP-ARKO Prostate

We detected the proliferative signals using Ki67 IHC staining and the apoptotic signal with TUNEL assay. It is known that the proliferative signals will be observed from birth till young adult ages. After adult stage, only few cells out of 1,000 are positive for proliferation signals. Therefore, the Ki67 staining was performed on prostates from mice at the age of 6 weeks. The quantitative Ki67 staining results (number of positive signals per 1,000 epithelial cells) showed that there is a significant reduction of Ki67 positive cells in VPs of FSP-ARKO mice (Fig. 3A). Again, it is well documented that the apoptotic signal is barely detectable in prostates of mice at a young age. The quantitative data from TUNEL apoptosis assay (number of positive signals per 1,000 epithelial cells) showed the increased apoptotic cells in VPs of FSP-ARKO mice at 24 weeks (Fig. 3B).

Reduced Expression Level of Collagen in the FSP-ARKO Prostate

Collagen, secreted by fibroblasts, could support the prostatic epithelial cells' proliferation [23]. Using Masson's trichrome staining [24, 25] and Picrosirius Red Staining [26], we determined the collagens expression level and found that there is a dramatically reduced collagen deposition in FSP-ARKO mouse prostate basement membrane especially at 6-weeksold (Fig. 3C and D), which might contribute to the defects of epithelium development and growth.

Decreased Stromal Factors and Luminal Epithelial Genes in the FSP-ARKO Prostate

Using Q-PCR, we examined the prostate stroma secreted factors and epithelial differentiation markers in the FSP-ARKO and WT mice at age of 6, 12, and 24 weeks. The data showed that loss of stromal AR resulted in the reduced expression of insulin-like growth factor-1 (IGF-1), fibroblast growth factor-7 (FGF-7), and fibroblast growth factor-10 (FGF-10) starting as early as 6-weeks-old, and hepatocyte growth factor (HGF) showed a reduced expression at 24 weeks in FSP-ARKO mice (Fig. 4A). We also found that several key genes expressed in differentiated epithelial cells, such as NKX3.1, PSP94, and Probasin (PB), were decreased in the prostate of 12- and 24-weeks-old FSP-ARKO mice (Fig. 4B), which indicated the defective epithelium differentiations in FSPARKO prostate were mediated by reduced stromal growth factors. Overall, the changes of stromal growth factors and luminal epithelial markers were consistent with the phenotype change.

AR Roles in the Primary Cultured Prostate Stromal Cells

To further confirm the in vivo findings in FSPARKO mice, we performed in vitro primary culture. We cultured the mouse prostate stromal cells (PrSCs), and stained the fibroblast marker (Vimentin) and smooth muscle marker (SMA) using immunofluorescence to confirm the cells' origin. As shown in Figure 5A, most of the cells are Vimentin and SMA double positive, but some of the cells are Vimentin single positive, which indicated the cells are a mixture of myofibroblasts and fibroblasts. To dissect the AR role in the PrSCs, we knocked down the AR using lentivirus AR-siRNA (PrSC-ARsi). The Q-PCR (Fig. 5B) and Western blot data (Fig. 5C) showed the PrSC-ARsi cells have reduced AR expression compared to control cells (PrSC-sc), and the MTT assay showed PrSC-ARsi cells grew slower than PrSC-sc cells (Fig. 5D). We then co-cultured the prostate epithelial BPH-1 cells with PrSC-ARsi or PrSC-sc cells, and found BPH-1 cells grew slower when co-cultured with PrSC-ARsi (Fig. 5E). To probe the possible mechanism, we screened some growth factors in PrSC-sc and PrSC-ARsi cells with Q-PCR, and found the decreased expressions of IGF-1, fibroblast growth factor-2 (FGF-2), FGF-7, fibroblast growth factor-9 (FGF-9), FGF-10, vascular endothelial growth factor-b (VEGFb), and placenta growth factor (PIGF) in PrSC-ARsi cells (Fig. 5F), but no change of VEGFc and Vimentin. It has been reported that FGF-2, FGF-9, VEGFb, and PIGF are all stromal secreted growth factors and contribute to the angiogenesis, stromal, and epithelial proliferation [27–30].

Together, the in vitro primary cell culture data indicated that the stromal AR might regulate the stromal cells proliferation and the secretory factors to further regulate the epithelial cell growth.

DISCUSSION

The prostate is an androgen target organ whose growth, morphogenesis, and functional maintenance are dependent on the androgen/AR signals [3, 31]. The stromal–epithelial interactions are critical for mediating the androgen/AR functions [6, 32]. The tissue recombination assays [9, 10] showed the stromal AR is critical for the prostate ductal morphogenesis, epithelial differentiation, and proliferation. However, the prostate stroma is not homogeneous and contains multiple cell types. The Cre-loxP system allows us to knock out the AR in selective cells, and to study the long-term effects of AR depletion in these cells.

In the present study, we established the FSP-ARKO mouse, and confirmed the AR knockout at DNA, mRNA, and protein levels. Although the gross appearance of prostate did not show an obvious difference, the histological analysis showed altered epithelial morphology with more cuboidal and flattened shapes in FSP-ARKO mouse, which indicates the impact of stromal cells on epithelial cells. Further assays showed the decreased proliferation, increased apoptosis, and defective expression of luminal epithelial genes including PSP94, NKX3.1, and probasin in FSP-ARKO mouse prostate. The above findings indicate the requirement of the stromal fibroblasts AR for the normal development and differentiation of prostate epithelium. Previously, Cunha's group reported that tissue recombinants composed of Tfm-UGM (without functional AR) and WT-epithelium failed to develop prostate [9, 10]. However, our FSP-ARKO mouse could develop prostates, though with some deficiencies.

There are three possible explanations to explain the differences: (1) In Tfm-UGM recombinants, the AR has no function in the whole stroma but in FSP-ARKO mouse, the AR is knocked out only in stromal fibroblasts; (2) the AR knockout efficiency in FSP-ARKO mouse fibroblasts is around 55–65%, the intact fibroblasts might compensate for the lower AR function to some degree; (3) tissue recombinants grow in the sub-renal capsule, where the physiological environments might be different from the prostate; there might be some unknown factors to contribute to the prostate development in prostatic physiological environments. Overall, although there are some differences, our findings in FSP-ARKO mouse are consistent with the previous tissue recombination results demonstrating that the stromal AR is essential for the normal prostate development.

We and other investigators have found and reported that the FSP1-cre knockout efficiency is around 55–65%. The FSP-1 cre has been used by an earlier report to knock out TGF beta receptor II (TBRII) [14]. They found that FSP-Cre could delete the floxed TBRII gene in fibroblasts as early as embryonic stage, yet the phenotypes of prostate intraepithelial neoplasia (PIN) was observed at a later age, suggesting the PIN lesion phenotype is also a sum accumulation of long time effects of TBRII loss. Since the knockout efficiency of fibroblast AR is not 100%, the reduced growth factors may still be sufficient to maintain the prostate structure at an early age. Thus, the phenotype change may not be clearly observed at an early time point. At 24 weeks, we observed more phenotype changes, which could be due to the continuing accumulation of the “partial defects” over the previous period.

It was reported that there is a periductal layer of fibroblastic cells in the proximal prostate ducts, in between the acinar basement membrane and periductal smooth muscle cells that also are AR-positive [33]. Based on tissue analyses and comparison, the periductal layer of fibroblastic cells are not frequently observed in our mouse prostate tissue sections. Accordingly, we did not observe that AR was profoundly lost in this type of fibroblast cells as compared to Wt littermate tissue sections. To date, there is no special cre available to selectively delete AR gene in this type of cells. Thus, it remains an interesting question to investigate whether AR plays a differential role in this periductal layer of fibroblastic cells.

The molecular pathways of stromal AR regulating prostate epithelial development and differentiation are mediated, at least in part, by growth factors secreted by the stromal cells under the influence of androgen signals [34]. Using the FSP-ARKO mice, we found that knockout of the stromal AR could down-regulate the FGF-10, FGF-7, and IGF-1 expression levels in prostate. Both FGF-10 and FGF-7 serve as paracrine growth factors synthesized exclusively in stromal cells and act through their receptor, FGFR2b, located in the epithelial cells for further action [35]. FGF-10 null mice could develop a urogenital sinus, but fail to develop prostate [36]. Although the FGF-7 null mouse showed little phenotype change [37], blocking the FGF-7 signals could inhibit androgen-stimulated prostatic epithelial growth and ductal branching [38]. IGF-1 plays an essential role in embryonic and postnatal development of multiple organs including the prostate [39, 40], and could be regulated by androgen/ AR at the transcriptional level via a potential ARE on its promoter [41]. The IGF-1 null mice developed smaller prostate with impaired glandular structures [40]. Furthermore, the IGF-1 was involved in the tumorigenesis, progression, and epithelial-to-mesenchymal transition of prostate cancer [42, 43].

These growth factors were further confirmed by the in vitro primary cultured prostate stromal cells. When knocking down the AR in PrSCs, we found more down-regulated genes including the FGF-2, FGF-9, VEGFb, and PIGF than in the in vivo setting. FGF-2, FGF-9, VEGFb, and PIGF could be produced from stromal cells and contribute to the prostate angiogenesis, as well as stromal and epithelial growth [27, 30]. The possible explanations for the in vivo and in vitro differences might be: the in vivo prostatic environment is quite complicated with complex cell–cell interaction, and other stromal cells might compensate for the lower expression of some growth factors; but the in vitro cell culture system could supply a relatively simple environment and pure cell population without compensation.

In the FSP-ARKO mice, we also found a dramatically reduced expression of collagens in the prostate basement membrane especially at 6-week-old (the reduced collagens were also observed at other stages, but not as dramatic as 6 weeks). Collagens, secreted by fibroblasts, are important components of the prostate extracellular matrix, and are also important in supporting the normal prostatic epithelial cells proliferation and differentiation [23]. It is reported that the prostatic collagen expression levels are regulated by androgen signals [44]. Castration could decrease the collagen content of the prostates of both prepubertal and adult rats, and androgens could stimulate the collagen expression in castrated rats [44]. These reports indicated that castration induced prostate epithelial shrinkage might be partly mediated by the decreased expression of collagen. Collagens were also reported to facilitate the colonization and growth of metastatic prostate cancer cells in the bone microenvironment [45], and to promote the proliferation of prostate cancer cells by regulating some related gene expressions [46]. Our data showed a significant reduced collagen expression in the FSP-ARKO mouse prostate, which might be another molecular mechanism by which stromal AR regulates the epithelium development and growth.

The fibroblasts and SMCs are two basic components of the prostate stroma. Recently, we have knocked out the AR in mouse SMCs (SM-ARKO) and obtained positive phenotypes [13]. Comparing the FSP-ARKO and SM-ARKO models (Fig. 6), we found the AR roles are distinct in these two models. (1) AR gene knockout in prostate lobes: Due to the special Cre expression preference, in the FSP-ARKO model, the AR is dominantly knocked out in the VP with 55– 65% efficiency; but in the SM-ARKO model, the AR is more dominantly knocked out in the anterior prostates. (2) Histological phenotype: In the FSP-ARKO model, the epithelial cells of the VPs are more cuboidal and flattened; in the SM-ARKO model, the APs have fewer epithelial infoldings into the lumens. (3) Growth factor profile: In the FSP-ARKO model, the IGF-1, FGF-7, FGF-10, and HGF are decreased; in the SM-ARKO model, only IGF-1 expression is decreased. (4) Proliferation vs. apoptosis: The proliferation rate is decreased in both models, but the increased apoptosis is only observed in FSP-ARKO mouse prostates. (5) Extracellular collagen deposition: The collagen deposition is reduced in FSP-ARKO prostates, but not in SM-ARKO prostates.

The majority of malignant prostate tumors arise as adenocarcinomas, which are derived from the epithelial cells. However, a growing body of evidence suggests that stromal fibroblasts might also play important roles in the prostate tumor initiation, progression, and metastasis [47, 48]. The stromal AR role in the prostate cancer is still controversial [21, 49, 50]. Based on our findings that the stromal AR could regulate the expression of a series of

growth factors and collagen deposition to mediate the epithelium growth and differentiation, there might be a potential to target the stromal AR for the prevention and treatment of prostate cancer.

Together, our study implies the importance of strommal fibroblast AR in the prostate development and cancer progression. A further understanding of AR roles in stromal fibroblast and detailed mechanisms of androgen/AR signaling between stroma and epithelium might lead to the development of therapeutic strategies with stromal AR as a target to treat prostate cancer.

CONCLUSIONS

Together, we found reduced proliferation and increased apoptosis in the FSP-ARKO prostate. Furthermore, the expression level of collagen, stromal factors, and luminal epithelial genes all decreased in our mouse model. We also used an in vitro model, the primary cultured prostate stromal cells, to study the mechanism and characteristics of stromal AR in prostate development. Our FSP-ARKO mice not only provide the first in vivo evidence for the requirement of stromal AR to maintain the development and homeostasis of the prostate, but may also suggest the selective knockdown of stromal AR may become a potential therapeutic approach to treat prostate cancer.

Acknowledgments

Grant sponsor: NIH; Grant numbers: DK60912 and CA122840; Sponsor: George H. Whipple Professorship Endowment; Grant sponsor: The National Science Council, Taiwan; Grant numbers: 96-2314-B-182A-023-MY2. 97-2314-B-182A-077-MY3.

REFERENCES

1. Jackson RS 2nd, Franco OE, Bhowmick NA. Gene targeting to the stroma of the prostate and bone. Differentiation. 2008; 76(6):606–623. [PubMed: 18494814]
2. Prins GS, Putz O. Molecular signaling pathways that regulate prostate gland development. Differentiation. 2008; 76(6):641–659. [PubMed: 18462433]
3. Chang C, Saltzman A, Yeh S, Young W, Keller E, Lee HJ, Wang C, Mizokami A. Androgen receptor: An overview. Crit Rev Eukaryot Gene Expr. 1995; 5(2):97–125. [PubMed: 8845584]
4. Galani A, Kitsiou-Tzeli S, Sofokleous C, Kanavakis E, Kalpini-Mavrou A. Androgen insensitivity syndrome: Clinical features and molecular defects. Hormones (Athens). 2008; 7(3):217–229. [PubMed: 18694860]
5. Yeh S, Tsai MY, Xu Q, Mu XM, Lardy H, Huang KE, Lin H, Yeh SD, Altuwaijri S, Zhou X, Xing L, Boyce BF, Hung MC, Zhang S, Gan L, Chang C. Generation and characterization of androgen receptor knockout (ARKO) mice: An in vivo model for the study of androgen functions in selective tissues. Proc Natl Acad Sci USA. 2002; 99(21):13498–13503. [PubMed: 12370412]
6. Thomson AA. Mesenchymal mechanisms in prostate organogenesis. Differentiation. 2008; 76(6): 587–598. [PubMed: 18752494]
7. Cunha GR, Alarid ET, Turner T, Donjacour AA, Boutin EL, Foster BA. Normal and abnormal development of the male urogenital tract. Role of androgens, mesenchymal-epithelial interactions, and growth factors. J Androl. 1992; 13(6):465–475. [PubMed: 1293128]
8. Cooke PS, Young P, Cunha GR. Androgen receptor expression in developing male reproductive organs. Endocrinology. 1991; 128(6):2867–2873. [PubMed: 2036966]

9. Cunha GR, Lung B. The possible influence of temporal factors in androgenic responsiveness of urogenital tissue recombinants from wild-type and androgen-insensitive (Tfm) mice. J Exp Zool. 1978; 205(2):181–193. [PubMed: 681909]
10. Cunha GR, Chung LW. Stromal-epithelial interactions-I. Induction of prostatic phenotype in urothelium of testicular feminized (Tfm/y) mice. J Steroid Biochem. 1981; 14(12):1317–1324. [PubMed: 6460136]
11. Takeda H, Lasnitzki I, Mizuno T. Change of mosaic pattern by androgens during prostatic bud formation in XTfm/X+ heterozygous female mice. J Endocrinol. 1987; 114(1):131–137. [PubMed: 3655602]
12. Wu CT, Altuwaijri S, Ricke WA, Huang SP, Yeh S, Zhang C, Niu Y, Tsai MY, Chang C. Increased prostate cell proliferation and loss of cell differentiation in mice lacking prostate epithelial androgen receptor. Proc Natl Acad Sci USA. 2007; 104(31):12679–12684. [PubMed: 17652515]
13. Yu S, Zhang C, Lin CC, Niu Y, Lai KP, Chang HC, Yeh SD, Chang C, Yeh S. Altered prostate epithelial development and IGF-1 signal in mice lacking the androgen receptor in stromal smooth muscle cells. Prostate. 2011; 71(5):517–524. [PubMed: 20945497]
14. Bhowmick NA, Chytil A, Plieth D, Gorska AE, Dumont N, Shappell S, Washington MK, Neilson EG, Moses HL. TGF-beta signaling in fibroblasts modulates the oncogenic potential of adjacent epithelia. Science. 2004; 303(5659):848–851. [PubMed: 14764882]
15. Placencio VR, Sharif-Afshar AR, Li X, Huang H, Uwamariya C, Neilson EG, Shen MM, Matusik RJ, Hayward SW, Bhowmick NA. Stromal transforming growth factor-beta signaling mediates prostatic response to androgen ablation by paracrine Wnt activity. Cancer Res. 2008; 68(12):4709–4718. [PubMed: 18559517]
16. Zhang C, Yeh S, Chen YT, Wu CC, Chuang KH, Lin HY, Wang RS, Chang YJ, Mendis-Handagama C, Hu L, Lardy H, Chang C. Oligozoospermia with normal fertility in male mice lacking the androgen receptor in testis peritubular myoid cells. Proc Natl Acad Sci USA. 2006; 103(47):17718–17723. [PubMed: 17095600]
17. Yeh S, Hu YC, Wang PH, Xie C, Xu Q, Tsai MY, Dong Z, Wang RS, Lee TH, Chang C. Abnormal mammary gland development and growth retardation in female mice and MCF7 breast cancer cells lacking androgen receptor. J Exp Med. 2003; 198(12):1899–1908. [PubMed: 14676301]
18. Niu Y, Altuwaijri S, Lai KP, Wu CT, Ricke WA, Messing EM, Yao, Yeh S, Chang C. Androgen receptor is a tumor suppressor and proliferator in prostate cancer. Proc Natl Acad Sci USA. 2008; 105(34):12182–12187. [PubMed: 18723679]
19. Mainwaring PN, Ellis PA, Detre S, Smith IE, Dowsett M. Comparison of in situ methods to assess DNA cleavage in apoptotic cells in patients with breast cancer. J Clin Pathol. 1998; 51(1):34–37. [PubMed: 9577369]
20. Ilio KY, Nemeth JA, Lang S, Lee C. The primary culture of rat prostate basal cells. J Androl. 1998; 19(6):718–724. [PubMed: 9876023]
21. Niu Y, Altuwaijri S, Yeh S, Lai KP, Yu S, Chuang KH, Huang SP, Lardy H, Chang C. Targeting the stromal androgen receptor in primary prostate tumors at earlier stages. Proc Natl Acad Sci USA. 2008; 105(34):12188–12193. [PubMed: 18723670]
22. Provenzano PP, Eliceiri KW, Campbell JM, Inman DR, White JG, Keely PJ. Collagen reorganization at the tumor-stromal interface facilitates local invasion. BMC Med. 2006; 4(1):38. [PubMed: 17190588]
23. Thornton M, Frederickson R, Mata L, Mawhinney M. Collagen and the proliferation and differentiation of rat ventral prostate epithelial cells. Biol Reprod. 1985; 33(1):213–227. [PubMed: 4063441]
24. Singh I. A modification of the Masson-trichrome stain. Indian J Pathol Bacteriol. 1969; 12(4):172–173. [PubMed: 4096983]
25. Chang JY, Kessler HP. Masson trichrome stain helps differentiate myofibroma from smooth muscle lesions in the head and neck region. J Formos Med Assoc. 2008; 107(10):767–773. [PubMed: 18926943]

26. Rodella LF, Rezzani R, Buffoli B, Bonomini F, Tengattini S, Laffranchi L, Paganelli C, Sapelli PL, Bianchi R. Role of mast cells in wound healing process after glass-fiber composite implant in rats. J Cell Mol Med. 2006; 10(4):946–954. [PubMed: 17125597]
27. Cross NA, Reid SV, Harvey AJ, Jokonya N, Eaton CL. Opposing actions of TGFbeta1 and FGF2 on growth, differentiation and extracellular matrix accumulation in prostatic stromal cells. Growth Factors. 2006; 24(4):233–241. [PubMed: 17381064]
28. Giri D, Ropiquet F, Ittmann M. FGF9 is an autocrine and paracrine prostatic growth factor expressed by prostatic stromal cells. J Cell Physiol. 1999; 180(1):53–60. [PubMed: 10362017]
29. Sordello S, Bertrand N, Plouet J. Vascular endothelial growth factor is up-regulated in vitro and in vivo by androgens. Biochem Biophys Res Commun. 1998; 251(1):287–290. [PubMed: 9790948]
30. Matsumoto K, Suzuki K, Koike H, Hasumi M, Matsui H, Okugi H, Shibata Y, Ito K, Yamanaka H. Placental growth factor gene expression in human prostate cancer and benign prostate hyperplasia. Anticancer Res. 2003; 23(5A):3767–3773. [PubMed: 14666676]
31. Heinlein CA, Chang C. Androgen receptor in prostate cancer. Endocr Rev. 2004; 25(2):276–308. [PubMed: 15082523]
32. Cunha GR, Cooke PS, Kurita T. Role of stromal-epithelial interactions in hormonal responses. Arch Histol Cytol. 2004; 67(5):417–434. [PubMed: 15781983]
33. Prins GS, Birch L. The developmental pattern of androgen receptor expression in rat prostate lobes is altered after neonatal exposure to estrogen. Endocrinology. 1995; 136(3):1303–1314. [PubMed: 7867585]
34. Berry PA, Maitland NJ, Collins AT. Androgen receptor signalling in prostate: Effects of stromal factors on normal and cancer stem cells. Mol Cell Endocrinol. 2008; 288(1–2):30–37. [PubMed: 18403105]
35. Katoh M. Cancer genomics and genetics of FGFR2 (Review). Int J Oncol. 2008; 33(2):233–237. [PubMed: 18636142]
36. Donjacour AA, Thomson AA, Cunha GR. FGF-10 plays an essential role in the growth of the fetal prostate. Dev Biol. 2003; 261(1):39–54. [PubMed: 12941620]
37. Guo L, Degenstein L, Fuchs E. Keratinocyte growth factor is required for hair development but not for wound healing. Genes Dev. 1996; 10(2):165–175. [PubMed: 8566750]
38. Cunha GR, Ricke W, Thomson A, Marker PC, Risbridger G, Hayward SW, Wang YZ, Donjacour AA, Kurita T. Hormonal, cellular, and molecular regulation of normal and neoplastic prostatic development. J Steroid Biochem Mol Biol. 2004; 92(4):221–236. [PubMed: 15663986]
39. Le Roith D. The insulin-like growth factor system. Exp Diabesity Res. 2003; 4(4):205–212. [PubMed: 14668044]
40. Ruan W, Powell-Braxton L, Kopchick JJ, Kleinberg DL. Evidence that insulin-like growth factor I and growth hormone are required for prostate gland development. Endocrinology. 1999; 140(5): 1984–1989. [PubMed: 10218945]
41. Wu Y, Zhao W, Zhao J, Pan J, Wu Q, Zhang Y, Bauman WA, Cardozo CP. Identification of androgen response elements in the insulin-like growth factor I upstream promoter. Endocrinology. 2007; 148(6):2984–2993. [PubMed: 17363459]
42. Kojima S, Inahara M, Suzuki H, Ichikawa T, Furuya Y. Implications of insulin-like growth factor-I for prostate cancer therapies. Int J Urol. 2009; 16(2):161–167. [PubMed: 19183230]
43. Li, Y.; Koeneman, KS. Insulin-like growth factor-I dependent upregulation of ZEB1 drives epithelial-to-mesenchymal transition in human prostate cancer cells. In: Graham, Tisheeka R.; Zhau, Haiyen E.; Odero-Marah, Valerie A.; Osunkoya, Adeboye O.; Sean Kimbro, K.; Tighiouart, Mourad; Liu, Tongrui; Simons, Jonathan W.; O'Regan, Ruth M., editors. Urol Oncol. Vol. 27. Department of Hematology and Oncology, Winship Cancer Institute, Emory University; Atlanta, GA; 2009. p. 112
44. Srinivasan N, Aruldhas MM, Govindarajulu P. Sex steroid-induced changes in collagen of the prostate and seminal vesicle of rats. J Androl. 1986; 7(1) 55-558.
45. Kiefer JA, Farach-Carson MC. Type I collagen-mediated proliferation of PC3 prostate carcinoma cell line: Implications for enhanced growth in the bone microenvironment. Matrix Biol. 2001; 20(7):429–437. [PubMed: 11691583]

46. Kiefer J, Alexander A, Farach-Carson MC. Type I collagen-mediated changes in gene expression and function of prostate cancer cells. Cancer Treat Res. 2004; 118:101–124. [PubMed: 15043190]

47. Ao M, Franco OE, Park D, Raman D, Williams K, Hayward SW. Cross-talk between paracrine-acting cytokine and chemo-kine pathways promotes malignancy in benign human prostatic epithelium. Cancer Res. 2007; 67(9):4244–4253. [PubMed: 17483336]

48. Ayala GE, Dai H, Tahir SA, Li R, Timme T, Ittmann M, Frolov A, Wheeler TM, Rowley D, Thompson TC. Stromal antiapoptotic paracrine loop in perineural invasion of prostatic carcinoma. Cancer Res. 2006; 66(10):5159–5164. [PubMed: 16707439]

49. Li Y, Li CX, Ye H, Chen F, Melamed J, Peng Y, Liu J, Wang Z, Tsou HC, Wei J, Walden P, Garabedian MJ, Lee P. Decrease in stromal androgen receptor associates with androgenindependent disease and promotes prostate cancer cell proliferation and invasion. J Cell Mol Med. 2008; 12(6B):2790–2798. [PubMed: 18266956]

50. Gao J, Isaacs JT. Development of an androgen receptornull model for identifying the initiation site for androgen stimulation of proliferation and suppression of programmed (apoptotic) death of PC-82 human prostate cancer cells. Cancer Res. 1998; 58(15):3299–3306. [PubMed: 9699659]

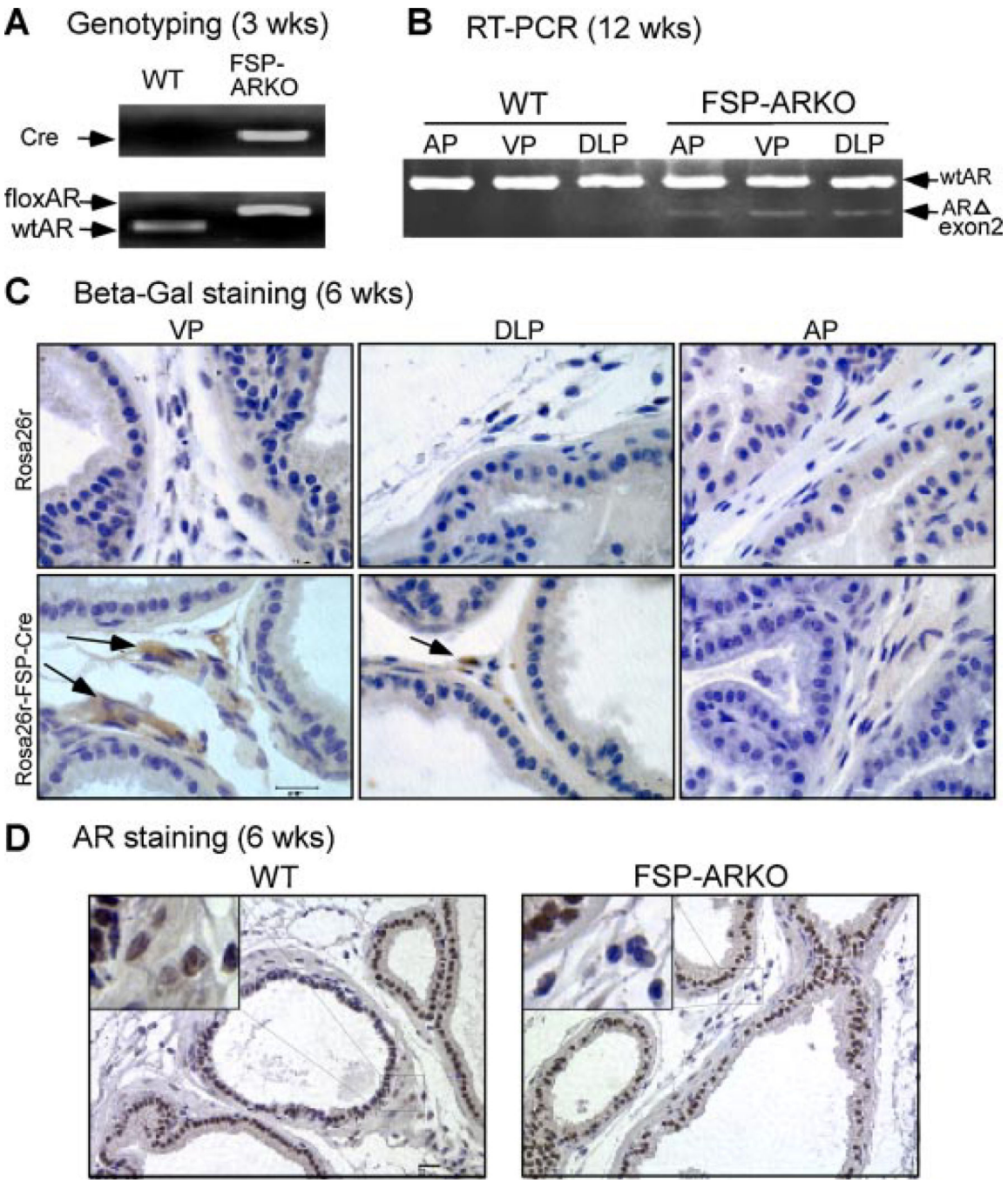

Fig. 1.

Generation and confirmation of FSP-ARKO mice. **A**: Genotyping indicated that Cre and floxed AR could be detected in the genomic DNA from tail snips of FSP-ARKO mice. **B**: Detection of the ARKO band at the RNA level. The primers located on exon 1and exon 3 of AR coding region were used to indicate the knockout of exon 2 gene by comparing PCR product size difference (WTAR band: 372 bp; exon 2 knockout band: 220 bp).**C**: ROSA26r-β-Gal mice were used to validate that FSP promoter drives the Cre expressed in the stromal compartment of prostate (VP, DLP, and AP). Arrows show positive cells by IHC staining,

and the highest Cre activity was observed in VP. Prostate stromal cells show efficient recombination and intensive staining accordingly, and the epithelial cells have no staining signal. **D**: AR IHC staining (using C19 antibody) was used to validate that AR gene was deleted in the VP of FSP-ARKO mice. (Scale bar = 20 μm).

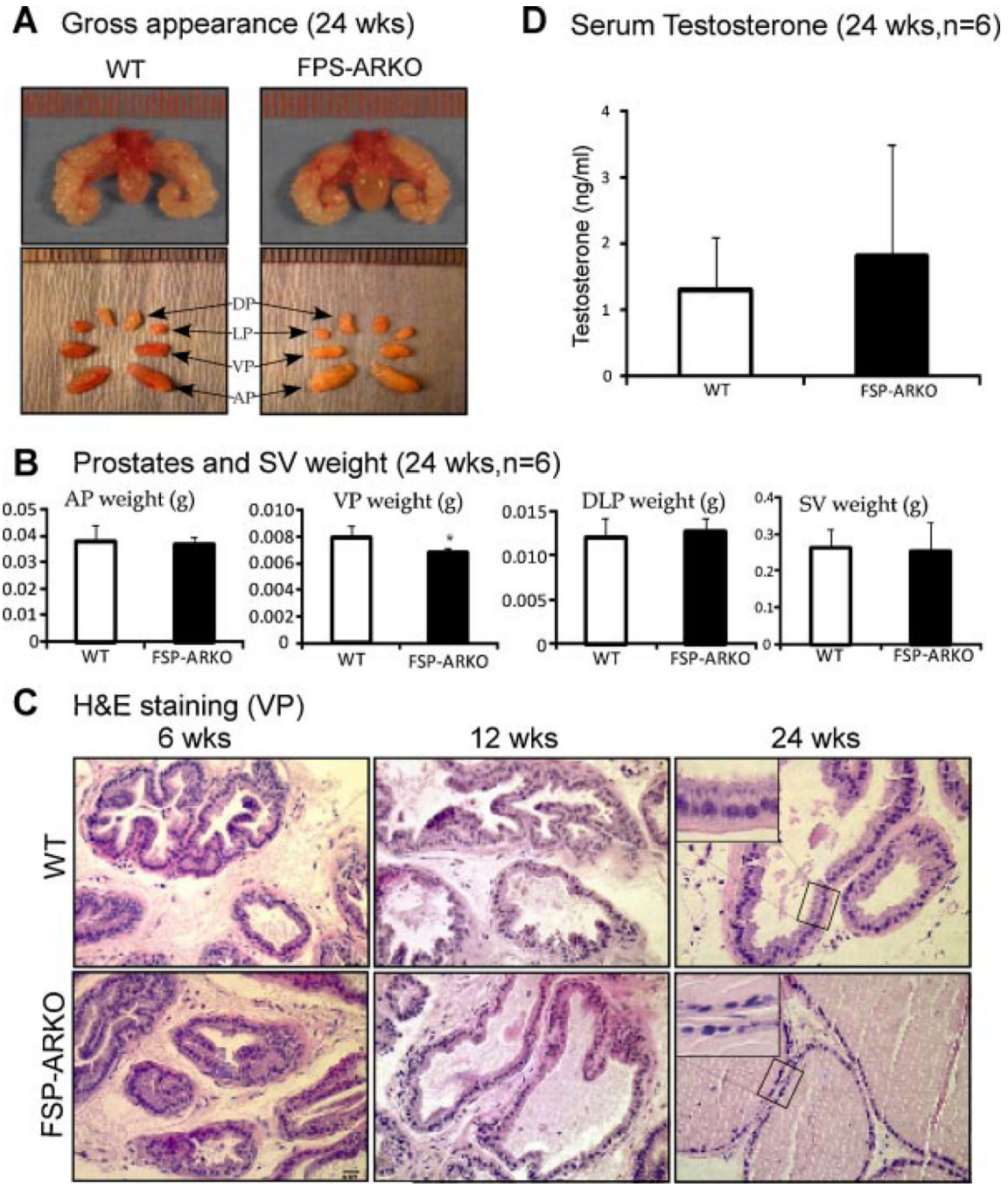

Fig. 2.

Phenotypes of prostate stromal ARKO (FSP-ARKO) mice. **A**: Comparable size and appearance of prostates from WT and FSP-ARKO male mice at age of 24 weeks (n = 6, arrows point to different prostate lobes). Left-upper: The gross appearance of the WT prostates; right-upper: The gross appearance of the FSP-ARKO prostates; left-lower: Different lobes of the WT prostates; right-lower: Different lobes of the FSP-ARKO prostates. **B**: Comparing the weights of the different lobes of prostates and seminal vesicles of WT and FSP-ARKO mice, only VPs have a significant reduction in FSP-ARKO mice, **P*

= 0.0350. **C**: Histological analyses of ventral prostates (VP) from WT and FSP-ARKO mice at the age of 6, 12, and 24 weeks. There is no change in the VP of FSP-ARKO mice at 6 weeks. We observed less folding structures at 12 weeks and altered epithelial cells with more cuboidal and flattened shapes in some area of prostate ducts in FSP-ARKO mice at 24-weeks; as a comparison, the WT prostates remain columnar shape (as shown at high magnification). Ten different fields of each mouse prostate were analyzed. Scale bar = 20 μm. **D**: Similar serum testosterone levels in WT and FSP-ARKO mice at 24-weeks-old: WT 1.3185 × 0.7835 ng/ml, FSP-ARKO 1.8225 × 1.6846 ng/ml, $P > 0.05$, n = 6 for each group.

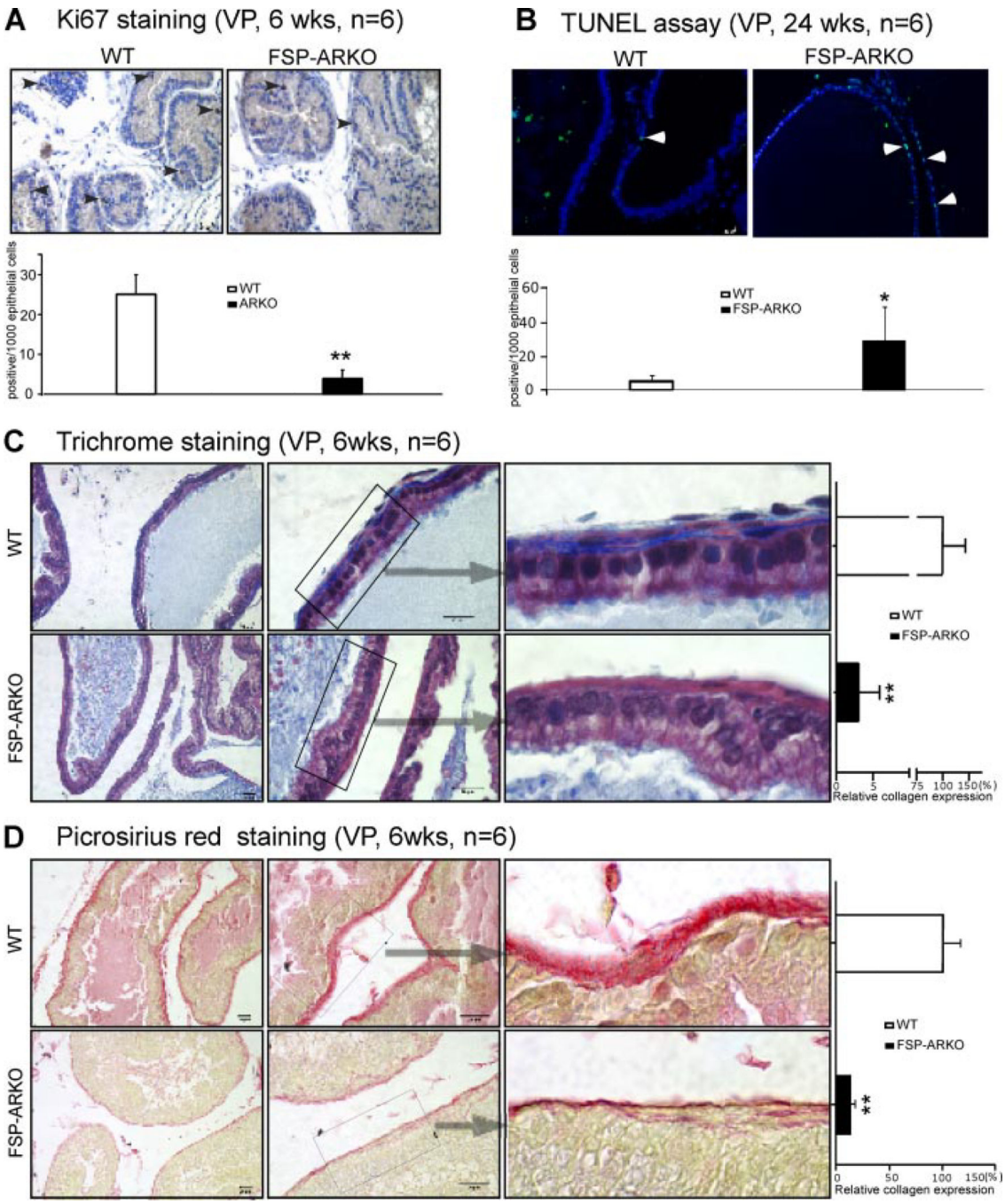

Fig. 3.

Alterations of proliferation, apoptosis, and collagen deposition in ventral prostates of FSP-ARKO mice. **A**: Ki67 IHC staining showed reduced proliferation rate in the prostate of FSP-ARKO mice as early as 6-weeks-old (arrowheads show positive Ki67 cells).Quantitative Ki67 signal was shown as the bar graph (Ki67 positive cells/1,000 epithelial cells). (**$P <$ 0.01 vs. WT littermates, n = 6). **B**: TUNEL assay showed increased apoptosis signals (green) in the prostate of FSP-ARKO mice at 24 weeks. (Arrowheads show positive apoptosis signals) The DAPI staining (blue) was used to indicate the location of nuclei.

Quantitatived at a were shown as the bar graph (positive apoptotic cells/1,000 epithelial cells). (*$P < 0.05$ vs. WT littermates, n = 6). **C**: Trichrome staining results suggested the reduced collagen surrounding the prostate ducts. Masson's trichrome staining of ventral prostate of FSP-ARKO mice (lower) and WT littermates (upper) at 6-weeks-old: The collagen (blue areas) in extracellular matrix (ECM) surrounding the ventral prostate epithelial acini decreased dramatically in the FSP-ARKO mice compared to WT littermates. The relative expression level of the collagen in WT mice was 100.00 ± 43.04%, but in FSP-ARKO mice it was only 3.05 ± 2.82% (**$P < 0.01$vs. WT littermates, n = 6. Scale bar = 20 μm). **D**: Picrosirius Red staining showed the reduced collagen (red color) surrounding the prostate ducts at 6-weeks-old FSP-ARKO mice (lower). The quantitative data was shown on the right lane: The relative expression level of the collagen in WT mice was 100.00 ± 16.46%, but in FSP-ARKO mice, it was only 13.64 × 3.21% (**$P < 0.01$ vs. WT littermates, n = 6, Scale bar = 20 μm).

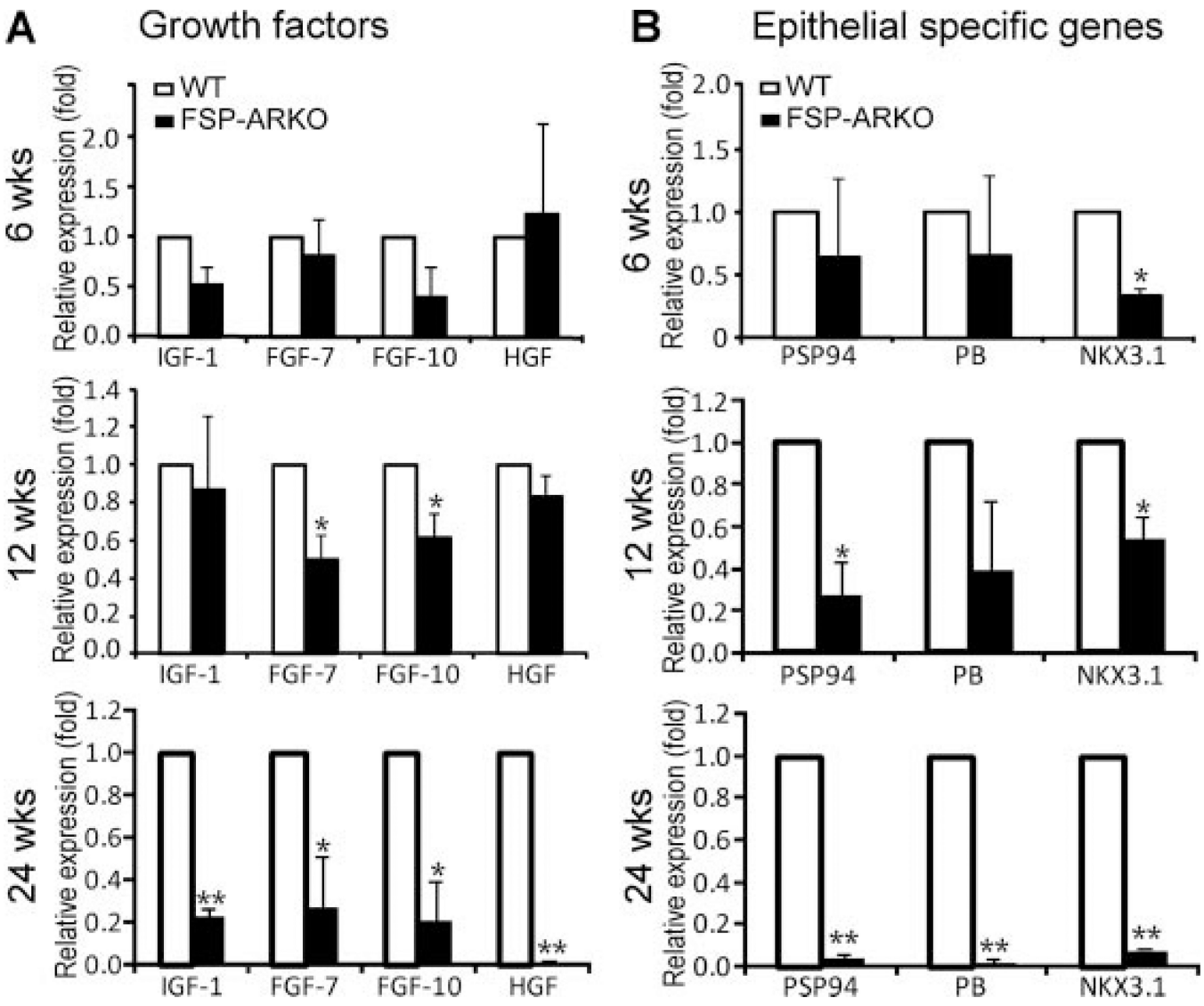

Fig. 4.

Growth factor expression profile in prostates of WT and FSP-ARKO mice. The expressions of (**A**) growth factors IGF-1, FGF-7, FGF-10, HGF, and (**B**) epithelial specific genes in the prostates of WT and FSP-ARKO mice at 6, 12, and 24 weeks were detected by Q-PCR. All the gene expression levels of FSP-ARKO mice were normalized by WT littermates (***P* < 0.01 vs. WT littermates, **P* < 0.05 vs. WT littermates; n = 4).

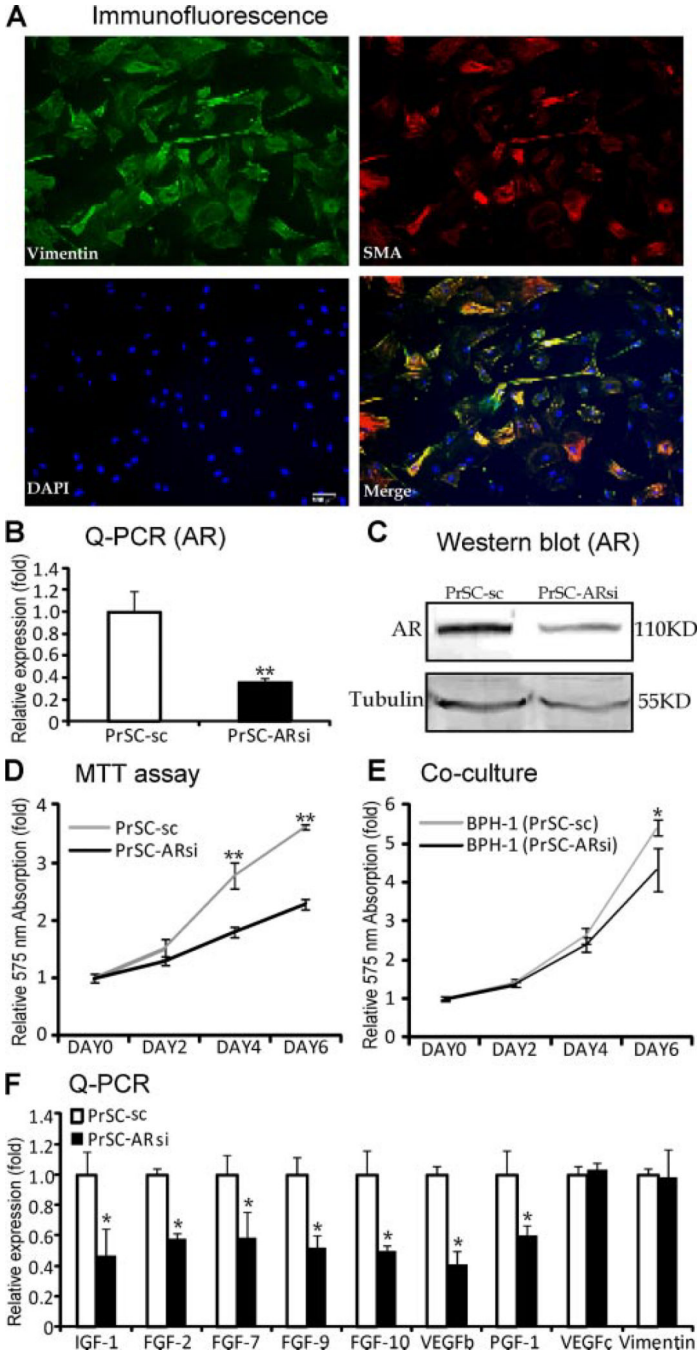

Fig. 5.

AR roles in the primary cultured prostate stromal cells. **A**: The immunofluorescence of vimentin (green) and SMA (red) in the primary cultured PrSCs. Scale bar = 100 μm. **B**: Reduced AR mRNA (left panel, Q-PCR) and (**C**) protein (right panel, Western blot) expression level in PrSC-ARsi cells, compared to PrSC cells. **D**: PrSC-ARsi cells showed lower growth rate than PrSC cells using MTT assay. **E**: BPH-1 cells co-cultured with PrSC-ARsi cells grew slower than those co-cultured with PrSC-sc cells using MTT assay. **F**: Decreased expressions of IGF-1, FGF-2, FGF-7, FGF-9, FGF-10,VEGFb, and PIGF, but not

VEGFc and Vimentin, in PrSC cells with AR knockdown (**$P < 0.01$vs. PrSC-sc, *$P < 0.05$ vs. PrSC-sc; n = 3).

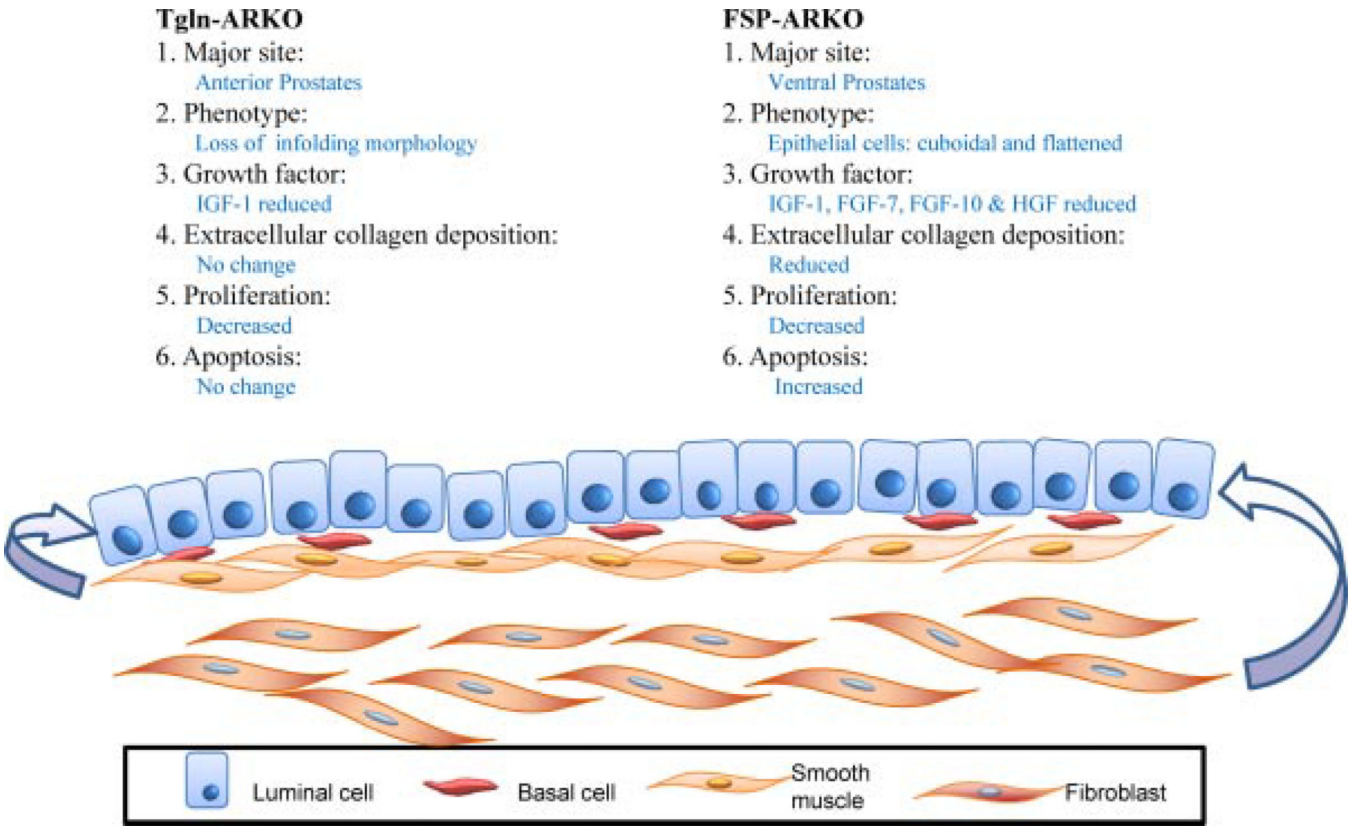

Fig. 6.

Comparison of FSP-ARKO and TGLN-ARKO mouse prostates. Our results suggest that AR roles are distinct in these two types of stromal cells. The cartoon summarizes the differences. (i) AR knockout efficiency: In the FSP-ARKO model, the AR is dominantly knocked out in the ventral prostates; but in the TGLN-ARKO model, the AR is more dominantly knocked out in the anterior prostates. (ii) The phenotype: In the FSP-ARKO model, the epithelial cells of the ventral prostates are more cuboidal and flattened; in the SM-ARKO model, the anterior prostates have fewer epithelial infoldings into the lumens. (iii) Growth factor profile: In the FSP-ARKO model, the IGF-1, FGF-7, FGF-10, and HGF are decreased; in the TGLN-ARKO model, only IGF-1 is decreased. (iv) Proliferation vs. apoptosis: The proliferation rate is decreased in both models, but the apoptosis level is increased only in FSP-ARKO mice, suggesting those changed stromal growth factors of FSP-ARKO could contribute to the growth and homeostasis of prostate. (v) Extracellular collagen deposition: The collagen deposition is reduced in FSP-ARKO prostates, but not in SM-ARKO prostates.

TABLE I

Primers for Q-PCR

Genes	Sense (5′-3′)	Anti-sense (5′-3′)
AR	GGACAGTACCAGGGACCATG	TCCGTAGTGACAGCCAGAAG
β-actin	ACCACACCTTCTACAATGAG	ACGACCAGAGGCATACAG
FGF-2	AACGGCGGCTTCTTCCTG	TGGCACACACTCCCTTGATAG
FGF-7	TCCTGCCAACTCTGCTCTAC	CTTTCACTTTGCCTCGTTTGTC
FGF-9	GGTCAGCATTCGTGGTGTG	CAGGTTGGAAGAGTAGGTGTTG
FGF-10	CTGCTGTTGCTGCTTCTTG	TGACCTTGCCGTTCTTCTC
HGF	AGAGGTACGCTACGAAGTC	GCTTGCCATCAGGATTGC
IGF-1	GGTGGATGCTCTTCAGTTC	TTTGTAGGCTTCAGTGGG
NKX3.1	GGTGATTGAGTTGGAGAGGAAG	GGTCTTATAGCGTCTGTTCTGG
PIGF	TCTGCTGGGAACAACTCAACA	GTGAGACACCTCATCAGGGTAT
Probasin	TCATCCTCCTGCTCACACTG	GACGGAAGTAGGTTCTCAATGG
PSP94	CACCTGCTGTACCAACGCTAC	GTTCTTCCGATCCACCACACTG
SMA	GCTTCGCTGGTGATGATG	GGTGATGATGCCGTGTTC
VEGFb	AAGCTGCTTTCCAGACTCCA	CTCACTTGACCAGGGTGGTT
VEGFc	GGAGGAAACCACGGGACAG	GAACACGCCAGAGACAAGAAG
Vimentin	CACACGCACCTACAGTCTG	GTCCACCGAGTCTTGAAGC